

Laminated, Composite and Sandwich Membranes Based on Graphene-Oxide with Nano-Textiles

Petra Roupцова^{1,2*}, Karel Klouda^{1,2}, Lucie Gembalova², Eva Kuzelova-Kostalova³ and Jiri Chvojka³

¹Research Institute for Occupational Health and Safety, Jeruzalemska 1283/9, Praha, 110 00, Czech Republic

²VSB-Technical University of Ostrava, Lumirova 13, Ostrava, 700 30, Czech Republic

³Technical University of Liberec, Studentska Liberec 1402/2, Liberec, 46117, Czech Republic

Abstract

The contribution describes preparation of graphene-oxide suspensions and their hybrid compounds, GO-biochar, GO-C₆₀, GO-CF_{0.9}, which are subsequently applied to nano-textiles using various techniques. This method was used to prepare composite and sandwich-type films or laminated nano-textiles. Relative arrangement in product (film) cross-sections was identified in products prepared using SEM analysis. Thermal stability of the products was determined using DTA, DSC analysis and compared to the stability of the nano-textiles. Chemical properties of graphene-oxide (GO) allow a number of its modifications, partial reduction, creation of composites with metals and their oxides. Preparation and thermal analysis GO-TiO₂/PCI /GO-TiO₂ has been described as an example. The conclusion of the project suggests possible application of the products (films).

Keywords: Nano-Textiles; Composite; Graphene

Introduction

GO membranes have laminar, layered structure with functional oxygenous epoxy, carboxyl, carbonyl or hydroxide groups, which induce the hydrophilic character of sp³ C-O (approx. 40%), while also containing the hydrophobic component sp²C=O [1].

There are possibilities of preparation for these membranes [1] such as smearing a drop of GO colloidal suspension over a smooth surface (SiO₂, polymer, paper etc.) via spray, vacuum filtering or the Langmuir-Blodgett method. GO membranes can only exist as a free-standing C-frame deposited either onto a different membrane and functionally connected with a polymer or modified into an “in situ” polymer matrix, creating a non-covalent or covalent composite connection [2-5], or onto a porous material [6-9].

Up until a certain level, the GO oxygenous functional group can be de-oxidized depending on the used reducing agent, preparing a compound that is commonly known in literature as rGO. This compound has increased thermal stability, hydrophobic character and increased capability of π-π interactions and defect (pore) creation within the carbonaceous grid frame. Graphene itself is a mono-atomic layer of carbon, undissolvable for any gases or solutions, while GO (rGO) with controlled defects exhibits great potential for application in filtering technology. For graphene, pores are purposefully created in the C-grid using directed electron rays, ion oxidization etching or oxygenous plasma. Pore size and acquired shape are published in the graphic concept [5,10]. Pore size and shape subsequently influence the application in Figure 1 [11], which shows the different progression of gas/ion separation for GO and graphene. Membranes based on graphene, GO, rGO are applied in the area of molecular separation, both in selective separation of gases, ions, small and ultra-small particles, desalination and purification of water, including disinfection [4,6,7,12-17].

The results of gas and ion separation are influenced by diffusion speed [18], layer investing [19], spacing between nano-particles of GO providing channels (Figure 1), gap size between the layers. The functional groups also expand separation abilities and possibilities. Examples of selective separation: CH₄/CO₂, CH₄/H₂S, CH₄/N₂, H₂/CO₂

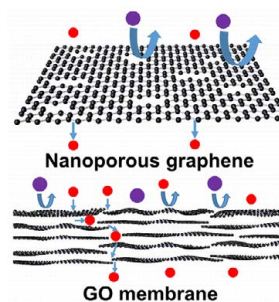


Figure 1: The porous membrane and the graphene stacked arrangement of GO membrane.



Figure 2: a) lamination and nanotextiles, b) composite.

*Corresponding author: Petra Roupцова, Research Institute for Occupational Health and Safety, Jeruzalemska 1283/9, Praha, 110 00, Czech Republic, Tel: 420774599992; E-mail: petra.roupcova@vsb.cz

Received: October 11, 2018; Accepted: October 22, 2018; Published: October 25, 2018

Citation: Roupцова P, Klouda K, Gembalova L, Kuzelova-Kostalova E, Chvojka J (2018) Laminated, Composite and Sandwich Membranes Based on Graphene-Oxide with Nano-Textiles. J Nanomed Nanotechnol 9: 517. doi: [10.4172/2157-7439.1000517](https://doi.org/10.4172/2157-7439.1000517)

Copyright: © 2018 Roupцова P, et al. This is an open-access article distributed under the terms of the Creative Commons Attribution License, which permits unrestricted use, distribution, and reproduction in any medium, provided the original author and source are credited.

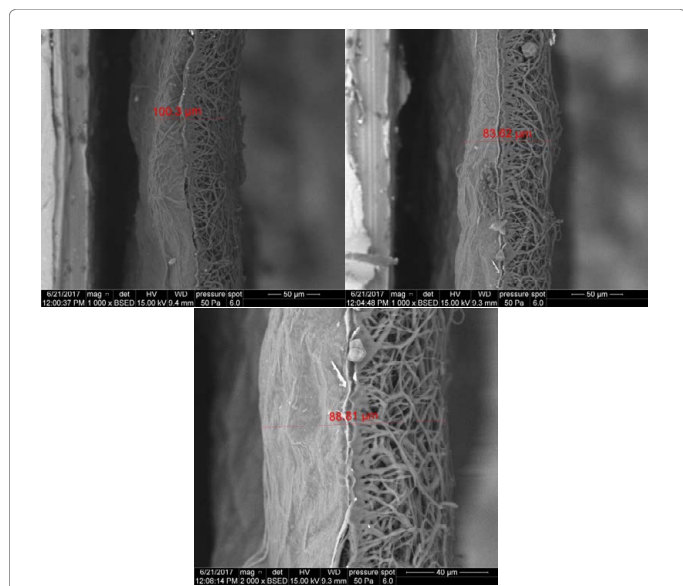


Figure 3: Sections of PCL nano-textile contact with GO applied (nano-textile lamination).

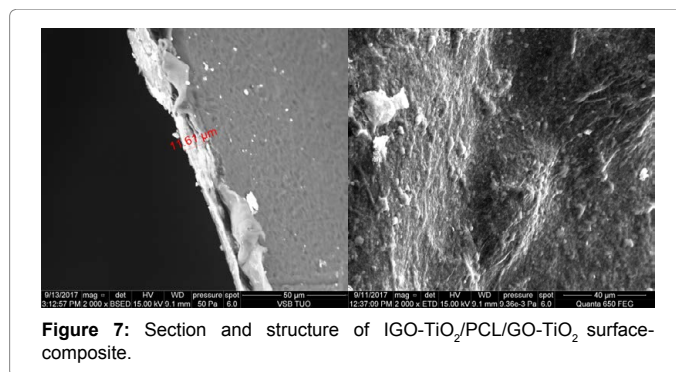


Figure 7: Section and structure of IGO-TiO₂/PCL/GO-TiO₂ surface-composite.

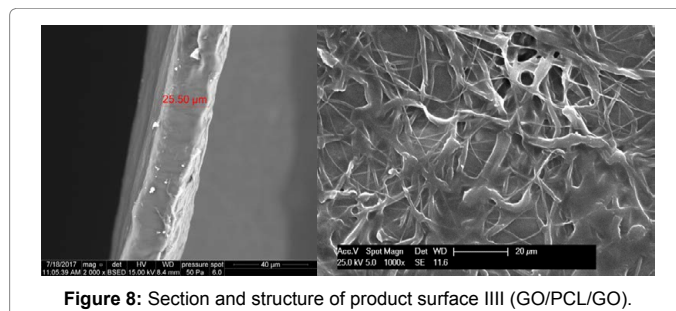


Figure 8: Section and structure of product surface III (GO/PCL/GO).

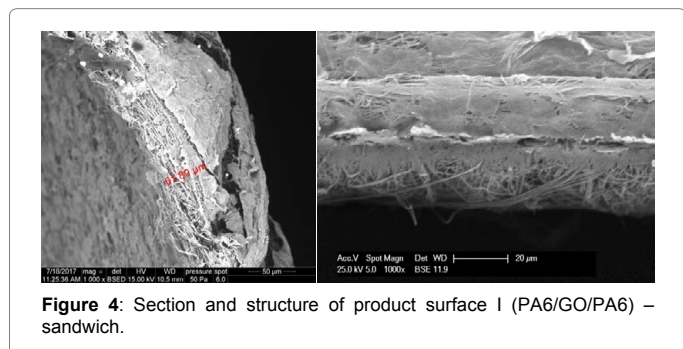


Figure 4: Section and structure of product surface I (PA6/GO/PA6) – sandwich.

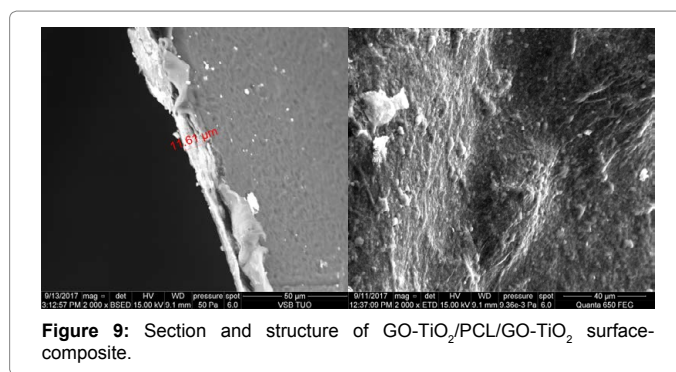


Figure 9: Section and structure of GO-TiO₂/PCL/GO-TiO₂ surface-composite.

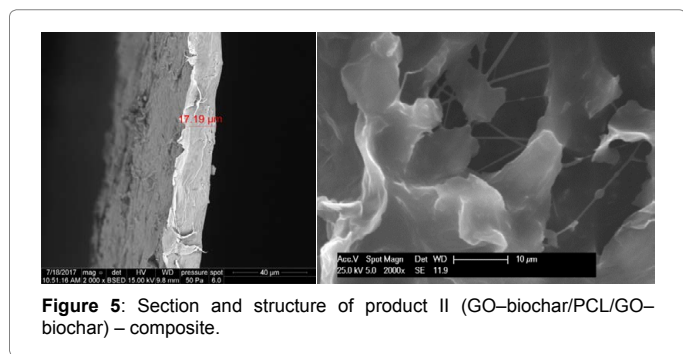


Figure 5: Section and structure of product II (GO–biochar/PCL/GO–biochar) – composite.

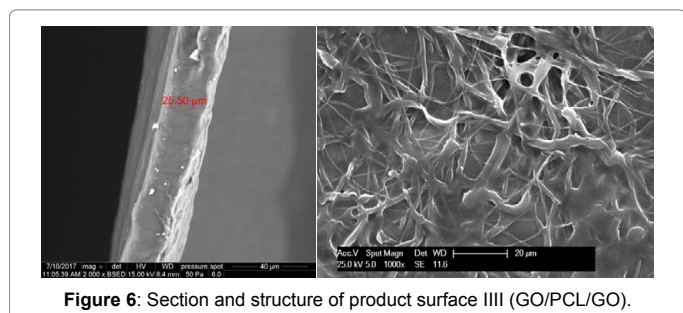


Figure 6: Section and structure of product surface III (GO/PCL/GO).

The next section shows pictures of sections and surfaces of selected film. The important property here is thermal resistance, which is presented by the TGA and DSC analysis curves.

Thermal analysis of default precursors

Thermal Analysis of precursors has been described through the Graph from Figures 10-13.

Thermal analysis result comparison -PA6/GO/PA6 sandwich against PA6 nano-textile (I)

Note the decomposition progression for the sandwich in Figure 14, where exo-effects are evenly alternated by endo-effect at temperatures from 150°C upwards, with the highest weight loss throughout the endo-effect progression. The entire sandwich decomposition ends in an exo-effect, peaking at 567°C with weight loss of 25%.

The decomposition of the PA6 nano-textile itself takes place from 150°C to 285°C in a protracted endo-effect and a 23% weight loss. The greatest weight loss (39 %) also occurs during an endo-effect at 430°C. There are two endo-effects on the curve Figure 12, the first one at 384°C with a 6% weight loss and the second one with main maximum at 515°C and weight loss of 19%. The GO influence manifested in warmer change

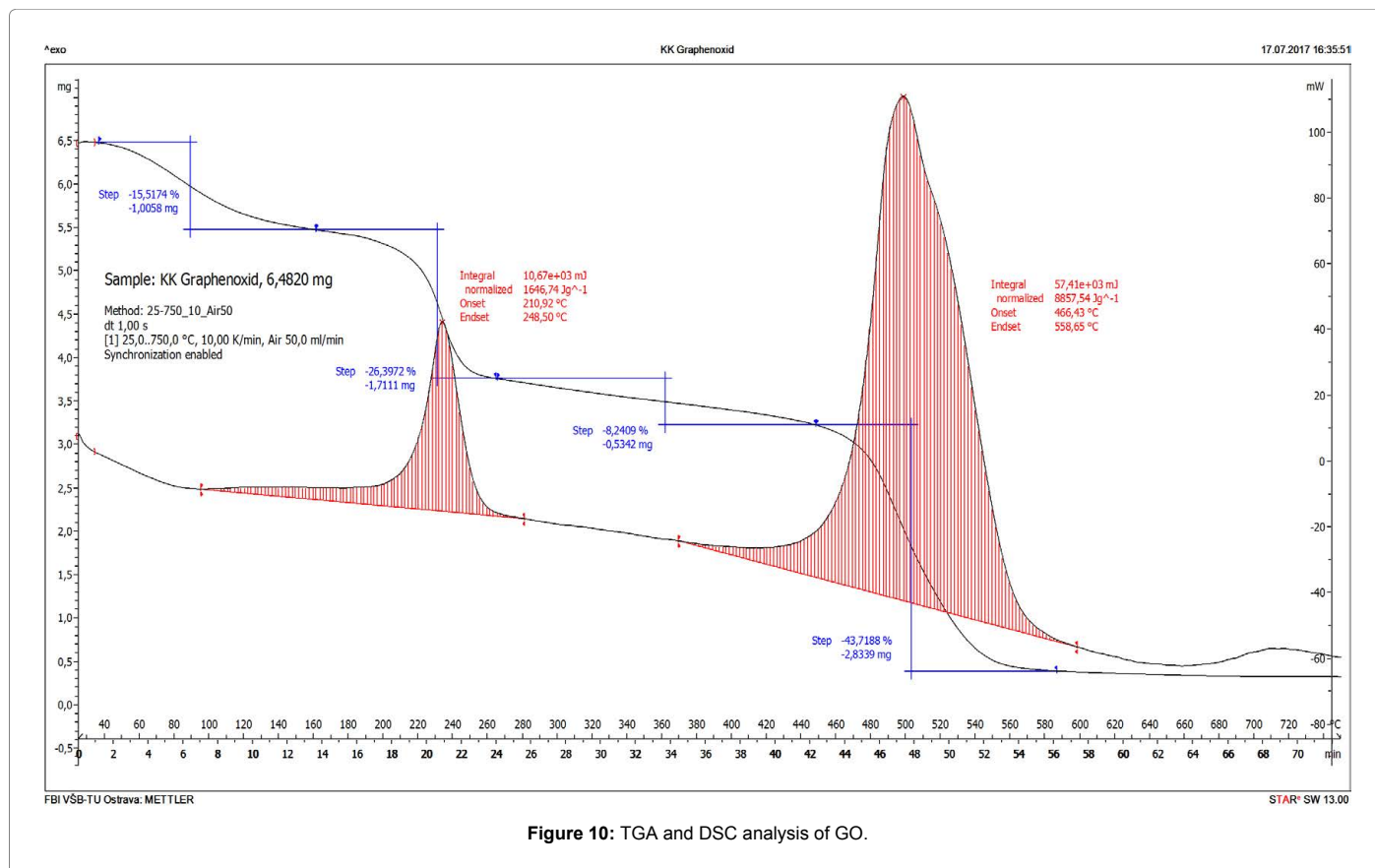


Figure 10: TGA and DSC analysis of GO.

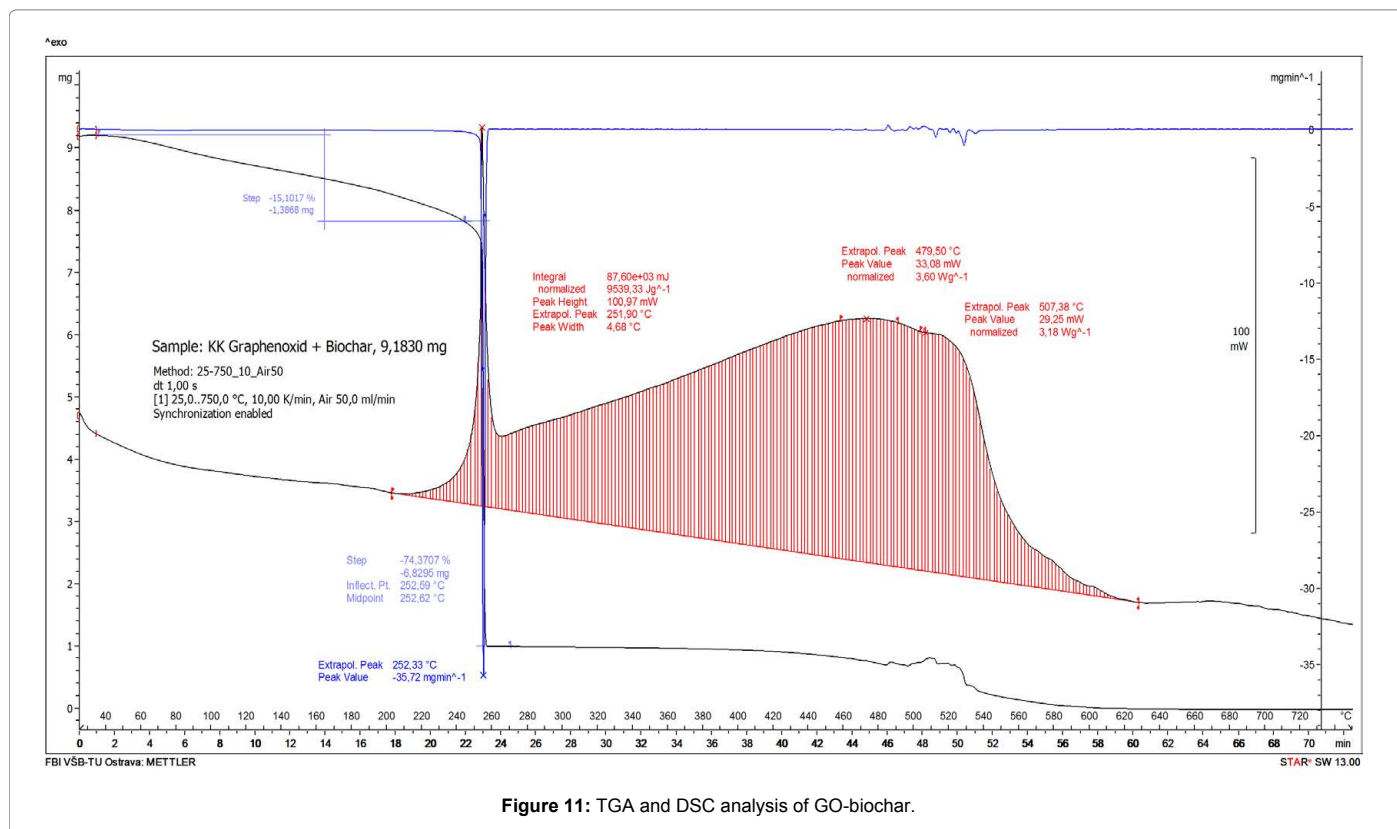


Figure 11: TGA and DSC analysis of GO-biochar.

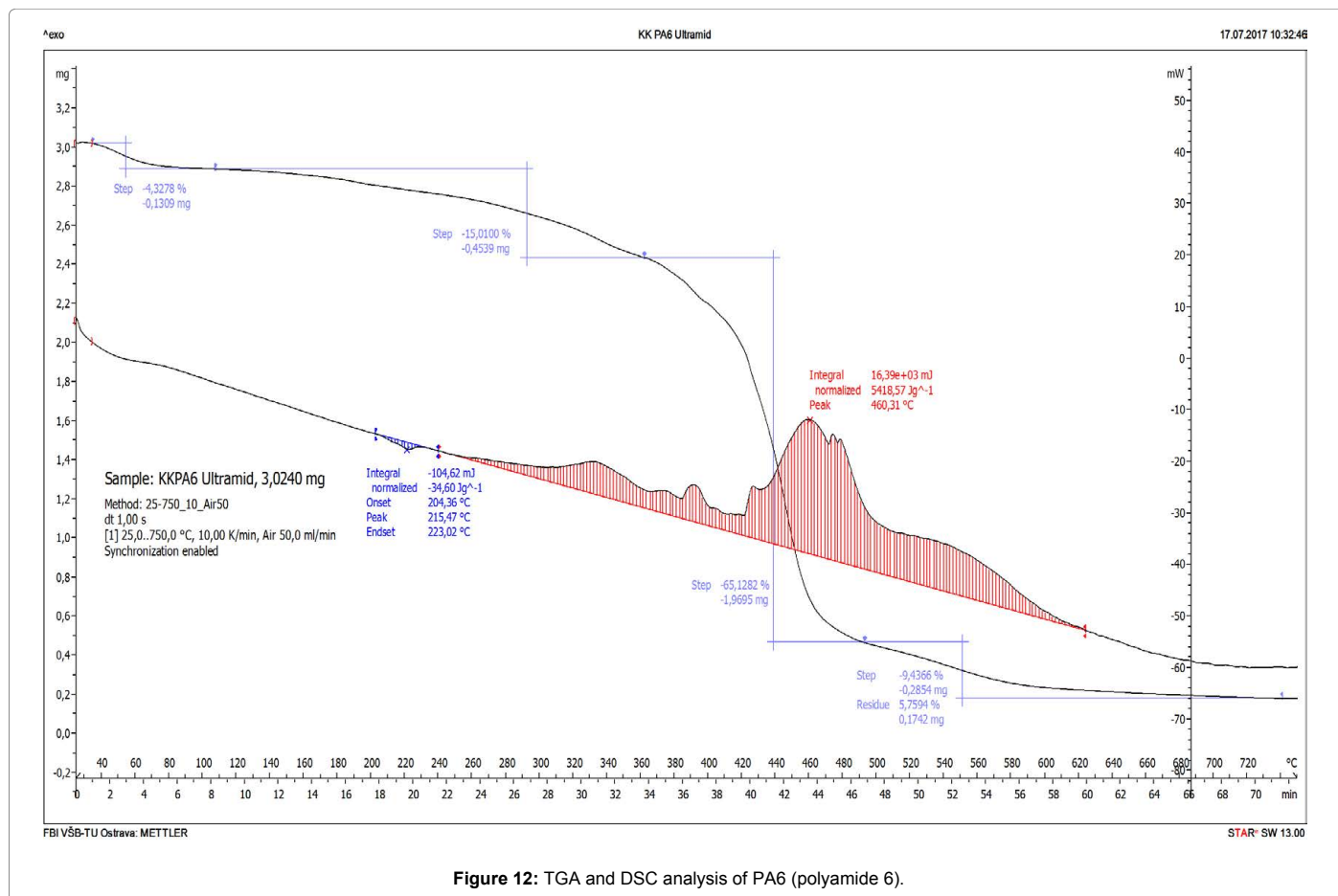


Figure 12: TGA and DSC analysis of PA6 (polyamide 6).

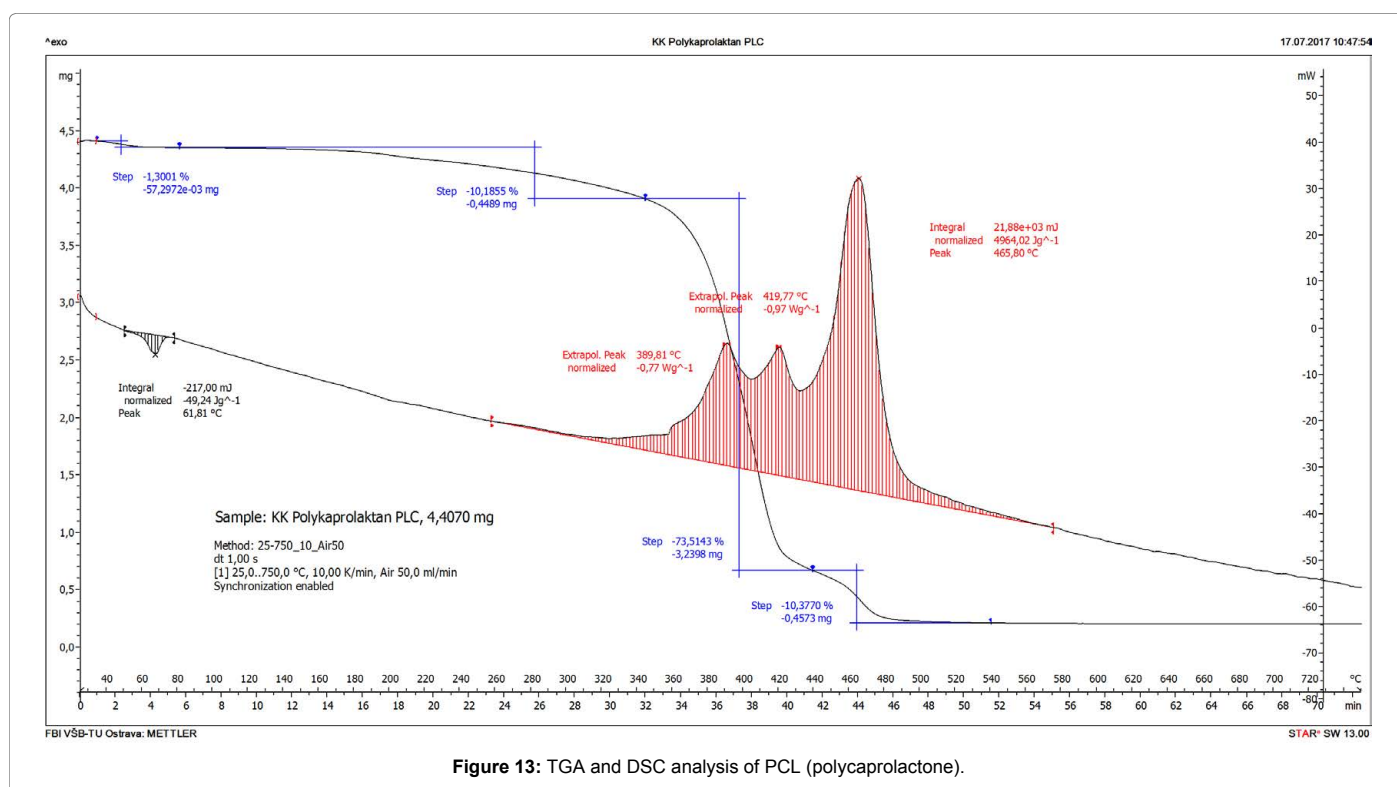


Figure 13: TGA and DSC analysis of PCL (polycaprolactone).

of the sandwich decomposition. The first and the last exo-effect in the sandwich are affected by the GO decomposition exo-effect. Mutual influence of these components is obvious in the created sandwich arrangement from the comparison of shape and progression of the TGA and DSL curves for the sandwiches with GO and nano-textiles.

Composite thermal analysis result comparison for GO-biochar/PCL/GO-biochar (II)

The measurement thermograph (Figure 15) was divided into three blocks within the range of 254–630°C -b), c) and d) with continuous exo-thermal change. Block b) peaks at 268°C, block c) ranges from 330 to 510°C with three hints of peaks and the high peak of the exo-effect was in block d) at 622°C. The highest weight loss (58 %) of the thermal decomposition has shown in block c).

The PCL decomposition itself happened in the thermal range of 260–580°C, with three identifiable exo-effects with maximums at 389°C, 410°C and 465°C. The main weight loss (73%) happened between the first and the second exo-effect (Figure 13). The PCL influence in the composite had mainly manifested in the protracted c) block. The hybrid compound effect had also manifested in block b), c) and partially d). When comparing the TGA and DSC of the starting components and the prepared composite, increased thermal stability can be clearly declared for the composite with a difference of 160°C, especially compared to the nano-textile.

Thermal analysis result comparison for the go/pcl/go (iii) composite and the caprolactam nano-textile

The measured thermograph was divided into three blocks in the temperature range of 150–600°C -b), c) and d), with mean temperature of 220°C for block b), temperature range of 265–480°C for block c), and mean temperature of 571°C for block d) (Figure 16).

The PCL decomposition itself happened in thermal range of 260–580°C, with three identifiable exo-effects with maximums at 389°C, 419°C and 465°C (Figure 13). The main weight loss (73%) happened between the first and the second exo-effect. The PCL influence in the composite had mainly manifested in the protracted c) block.

Thermal stability of the composite had increased by 100°C compared to the nano-textile (PCL) and the thermal change of the range for the last exo-effect. 30°C for the composite, 100°C for PCL, which is why we can expect mutual physical or chemical influence between the polymer and GO.

Composite thermal analysis result comparison for GO-TiO₂/PCL/GO-TiO₂

The comparison of thermograph curves for the GO/PCL/GO composite alone and composite containing TiO₂ has shown a difference in the thermal decomposition progression. The significant difference can be seen on the TGA curve in the last third of the decomposition (Figures 16-19). The decomposition of the TiO₂ composite starts ca. 30°C later and the maximum of the last exo-effect was 70°C lower; despite that the thermal change of the decomposition reaction of this exo-effect had doubled.

It is obvious that the TiO₂ content had played a part in the thermal properties of GO-TiO₂/PCL/GO-TiO₂. According to literature [23] TiO₂ is expected to be wrapped into plates of GO using hydroxy groups on the surface of GO leads to the Ti-O-C configuration.

Meltblown technology

A Meltblown technology was used to prepare a further type of sandwich arrangement between GO-Biochar and non-woven textiles. With this technology, polypropylene (PP) fabrics (Mostek) produced fiber

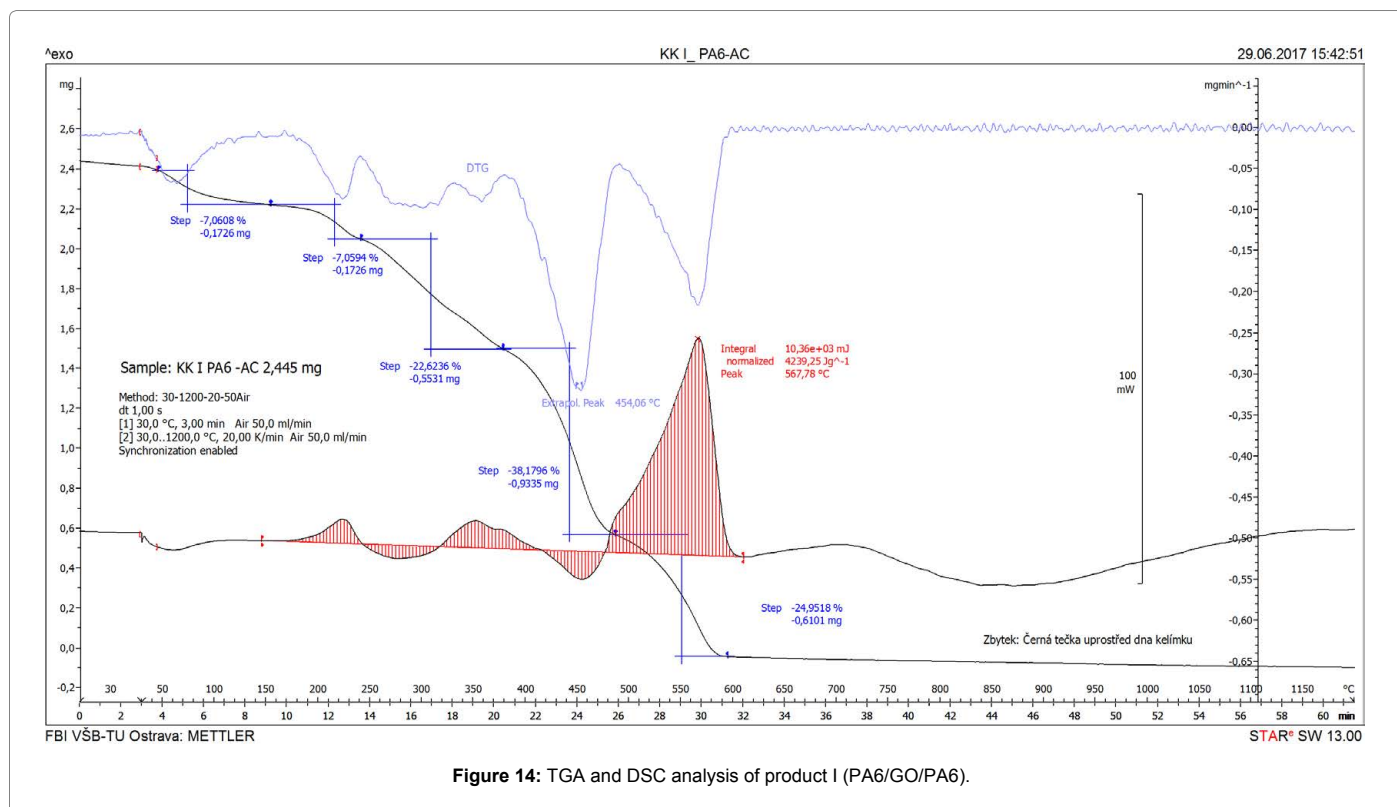


Figure 14: TGA and DSC analysis of product I (PA6/GO/PA6).

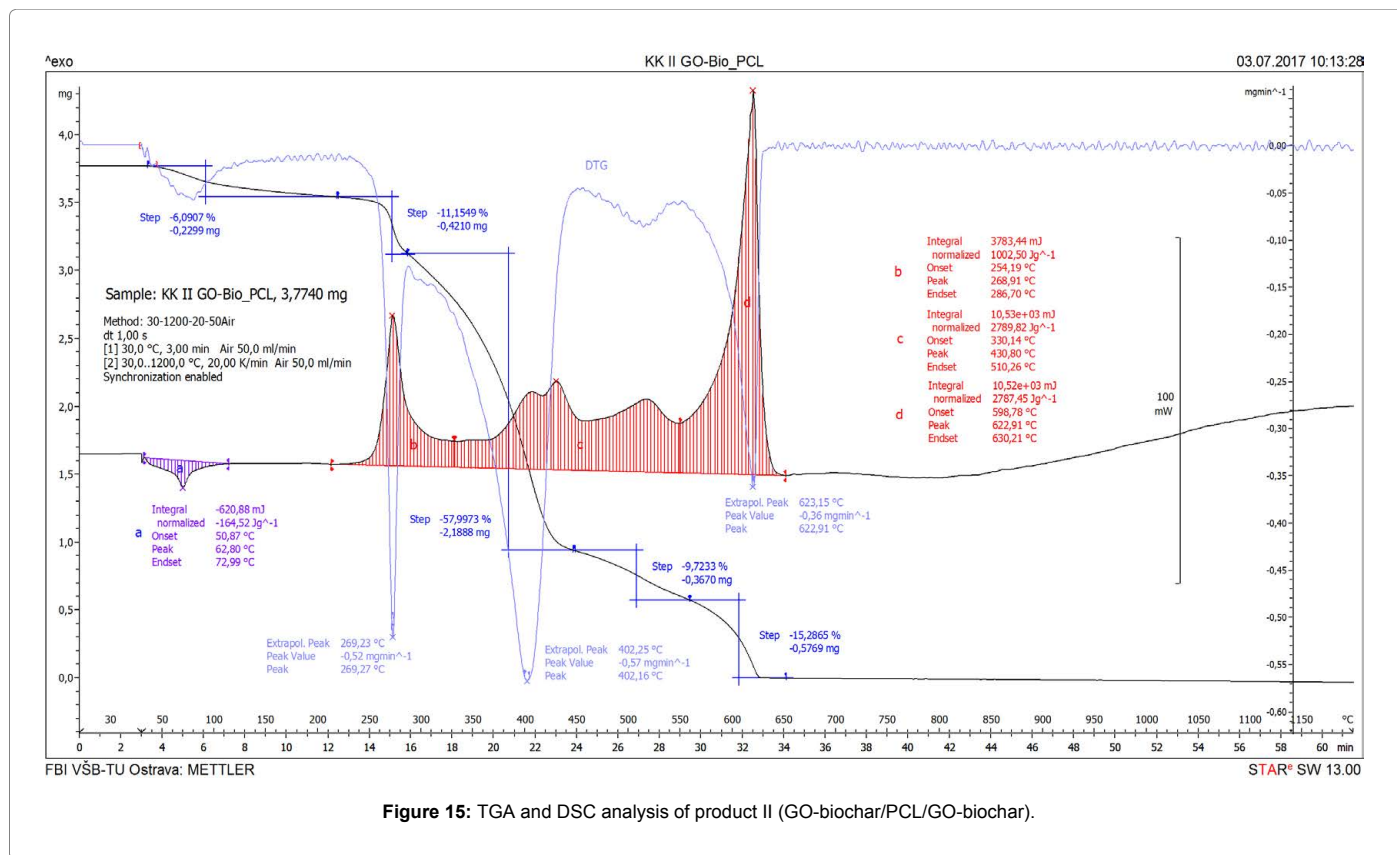


Figure 15: TGA and DSC analysis of product II (GO-biochar/PCL/GO-biochar).

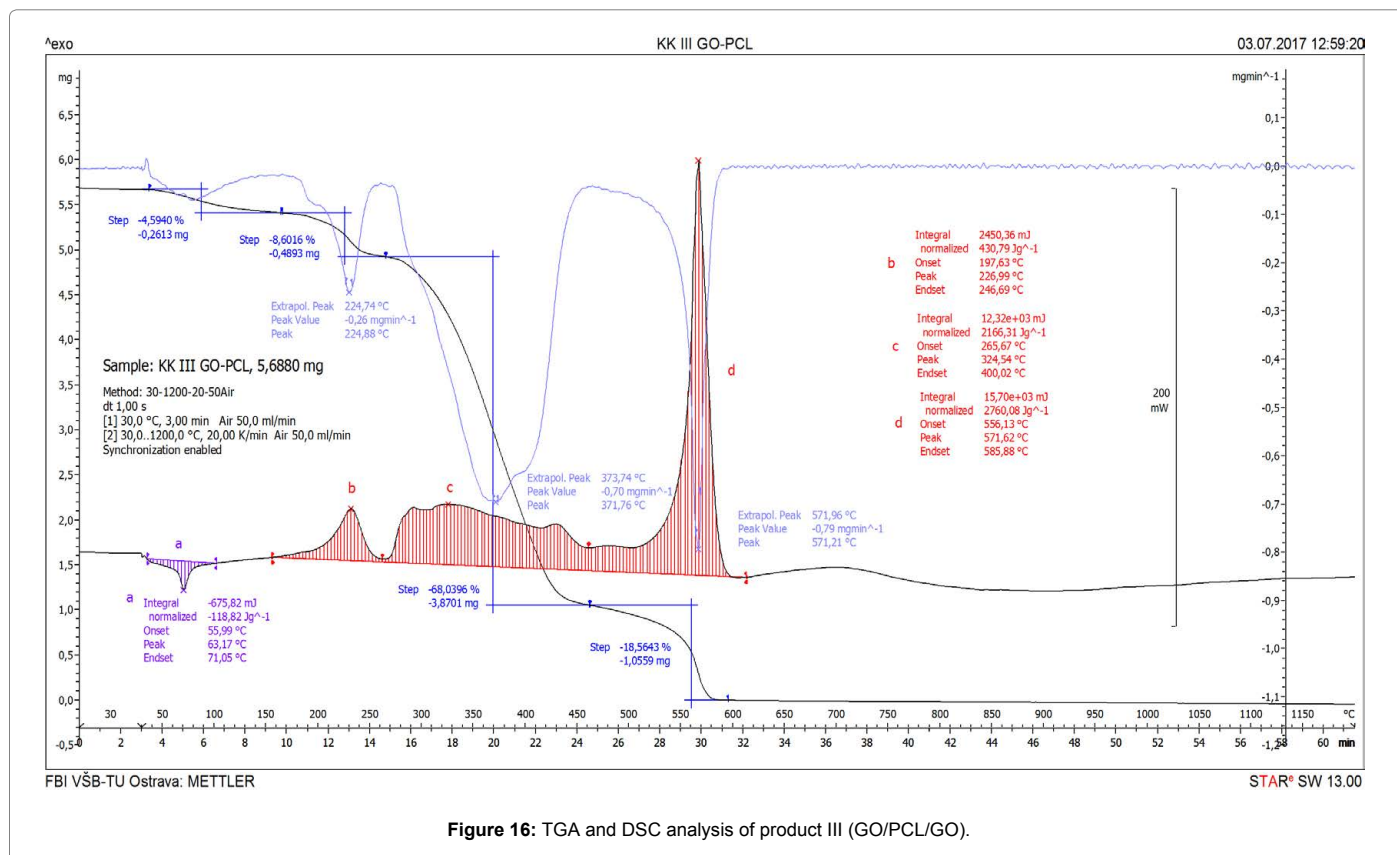


Figure 16: TGA and DSC analysis of product III (GO/PCL/GO).

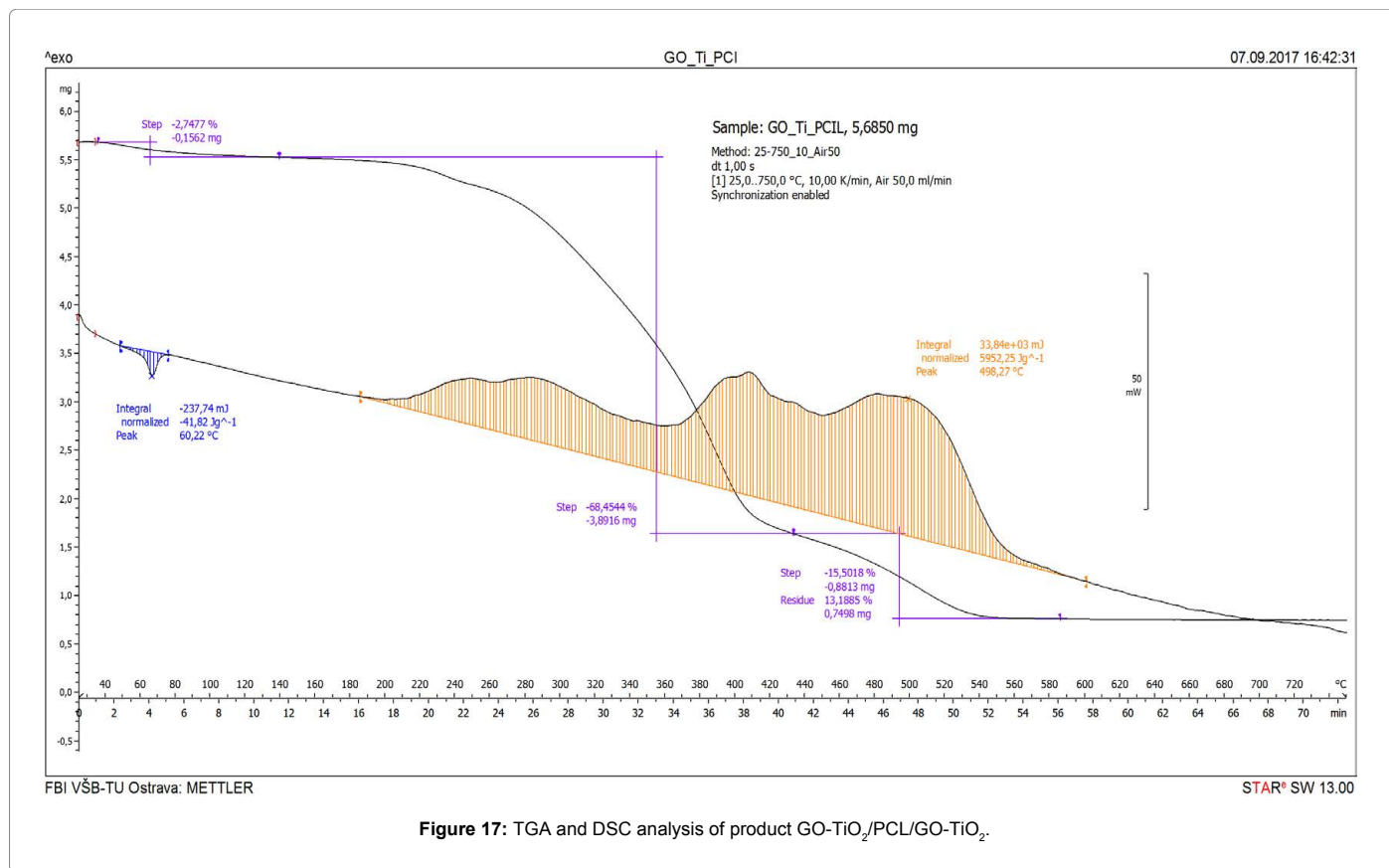


Figure 18: Prepared sandwich with biochar by Meltblown PP technology.

fabrics, which were doped with powder GO, GO-Biochar (2:1) and the biochemistry itself. Subsequently this deposited fabric was coated with nanoparticle with PCl and laminated (Figure 16) (where is shown cut out of the prepared foil by *Meltblown* technology on the left which was further tested).

This prepared material was tested according to Czech Technical Standart CSN EN 149: 2002 + A1: 20009 Respiratory protective devices on the cuts with adsorbent of the doped parts and parts without adsorbent.

Specific measuring instruments:

- INSPEC breathing resistance test device;
- Sheffield head;
- Manometer GDH 200-07;
- Yokogawa P052 Rotameter;
- Yokogawa P161 Rotameter;
- Stopwatch Ruhla;
- Thermometer type Centigrade 0.1;
- LORENZ type BIA paraffin oil aerosol filter device;
- Aerosol NaCl Testing Unit, MOORE'S Type 1100;

Metrological provision

The metrological provision of the instruments is performed in accordance with the Research Laboratory of Occupational health and Safety- metrology regulations (VÚBP-Praha).

Test results of prepared membranes (Tables 1 and 2)

100% = ADF 62

A, B = the samples with coating

C = A sample without coating

160 -biochar

150 -GO-biochar

200 -GO

Best results against air resistance were achieved for the biochar membrane prepared by *meltblown* technology on non-woven fabrics from PP.

Conclusion

Products prepared using graphene oxide and its nano-textile hybrids (PCI, PA6) feature higher thermal stability than the default nano-textiles. Suspension consistence/ composition and nano-textile porousness can influence which connection is established and therefore which particular product is prepared. The mutual link and



Figure 19: Measurement device for respiratory resistance and aerosol penetration for NaCl and paraffin oil (a) Sodium chloride test - Breakthrough of NaCl after 3 minutes. Flow rate 45 l/min.

Sample	State	Resistance in Pa	
		During 30 l/min	During 95 l/min
200A-GO	AR	1925	-
200B-GO	AR	1844	4920
200C-GO	AR	6.5	39
160A- biochar	AR	2230	3820
160B-biochat	AR	2150	3930
160C-biochar	AR	3	33
150A-GO-biochar	AR	1965	2710
150B-GO-biochar	AR	1971	2820
150C-GO-biochar	AR	4	35

Note: Values 150, 160 and 200 in the table and following table indicate the weight of the powder (adsorbent) per m²

Table 1: Determination of respiratory resistances.

Sample	State	Penetration %
200B-GO	AR	<1 x 10 ⁻³
200C-GO	AR	98
160B-biochar	AR	<1 x 10 ⁻³
160C-biochar	AR	96
150B-GO-biochar	AR	<1 x 10 ⁻³
150C-GO-biochar	AR	99

(a) Paraffin oil test - Breakthrough of paraffin oil after 3 minutes, flow rate 95 l / min.

Sample	State	Penetration %
200A-GO	AR	0
200C-GO	AR	93.1
160A-biochar	AR	0
160C-biochar	AR	93.1
150A-GO-biochar	AR	0
150C-GO-biochar	AR	96.5

(b) Sodium chloride test - Breakthrough of NaCl after 3 minutes. Flow rate 45 l /min

Table 2: Determination of aerosol penetration.

combination of components, along with further graphene oxide modification, provide high application flexibility namely in electrical engineering as a membrane or sensor material, as well as adsorption or anti-bacterial material. Article shows the potential application of GO, Biochar and hybrid GO-Biochar with PP microfibers as an adsorptive material for the measurement of the respiratory resistance and aerosol penetration for certain substances (NaCl, paraffin oil).

References

1. Huang H, Ying Y, Peng X (2014) Graphene oxide nanosheet: an emerging star material for novel separation membranes. *J Mat Che A* 2: 13772-13782.
2. Zinadini S, Zinatizadeh AA, Rahimi M, Vatanpour V, Zangeneh H (2014) Preparation of a novel antifouling mixed matrix PES membrane by embedding graphene oxide nanoplates. *J Memb Sci* 453: 292-301.
3. Chae H, Lee J, Lee C, Kim I, Park P (2015) Graphene oxide-embedded thin-film composite reverse osmosis membrane with high flux, anti-biofouling, and chlorine resistance. *J Memb Sci* 483: 128-135.
4. Hegab HM, Zou L (2015) Graphene oxide-assisted membranes: Fabrication and potential applications in desalination and water purification. *J Memb Sci* 484: 95-106.
5. Yoo BM, Shin HJ, Yoon HW, Park HB (2013) Graphene and Graphene Oxide and Their Uses in Barrier Polymers. *Inc J Appl Polym Sci* 131: 39628-39650.
6. Fatemi SM, Abbasi Z, Rajabzadeh H, Hashemizadeh SA, Deldar AN (2017) A review of recent advances in molecular simulation of graphene-derived membranes for gas separation. *Springer* 71: 194.
7. Akbari A, Sheath P, Martin ST, Shinde DB, Shaibani M, et al. (2016) Large-area graphene-based nanofiltration membranes by shear alignment of discotic nematic liquid crystals of graphene oxide. *Nat Commu*.
8. <https://pubs.acs.org/doi/abs/10.1021/acsnano.5b07304>
9. Woo YC, Tijing LD, Shim WG, Choi JS, Kim SH, et al. (2016) Water desalination using graphene-enhanced electrospun nanofiber membrane via air gap membrane distillation. *J Memb Sci* 520: 99-110.
10. Huang L, Zhang M, Li C, Shi G (2015) Graphene-Based Membranes for Molecular Separation. *J Phys Chem Lett* 6: 2806-2815.
11. You Y, Sahajwalla V, Yoshimura M, Joshi RK (2016) Graphene and graphene oxide for desalination. *Nanoscale* 8: 117-119.
12. Dervin S, Dionysiou DD, Pillai SC (2016) 2D nanostructures for water purification: graphene and beyond. *Nanoscale* 8: 15115-15131.
13. Aghigh A, Alizadeh V, Wong HY, Islam S, Amin N, et al. (2015) Recent advances in utilization of graphene for filtration and desalination of water: A review. *Desalination* 365: 386-397.
14. Han Y, Xu Z, Gao C (2013) Ultrathin Graphene Nanofiltration Membrane for Water Purification. *Adv Func Mat* 23: 3693-3700.
15. Lawler J (2016) Incorporation of Graphene-Related Carbon Nanosheets in Membrane Fabrication for Water Treatment: A Review. *Membranes* 4: 57.
16. Jiao S, Xu Z (2015) Selective Gas Diffusion in Graphene Oxides Membranes: A Molecular Dynamics Simulations Study. *ACS Appl Mater Interfaces* 7: 9052-9059.
17. Tanugi DC, Grossman JC (2012) Water Desalination across Nanoporous Graphene. *Nano Lett* 12: 3602-3608.
18. Kim D, Kim DW, Lim HK (2014) Intercalation of Gas Molecules in Graphene Oxide Interlayer: The Role of Water. *J Phy Chem C* 118: 11142-11148.
19. Sun C, Wen B, Bai B (2015) Application of nanoporous graphene membranes in natural gas processing: Molecular simulations of CH₄/CO₂, CH₄/H₂S and CH₄/N₂ separation. *Che Eng Sci* 138: 616-621.
20. Kim HW, Yoon HW, Yoon SM, Yoo BM, Yoo BM (2003) Selective Gas Transport Through Few-Layered Graphene and Graphene Oxide Membranes. *Science* 342: 91-95.
21. Fatemi FS, Arabieh M, Sepehrian H (2015) Nanoporous graphene oxide membrane and its application in molecular sieving. *Carbon lett* 16: 183-191.
22. Mahmood FS, Hamid S, Masoud A (2016) Selective Nanopores in Graphene Sheet for Separation I-129 Isotope from Air. *J Adv Phy* 5: 1-8.
23. Chao C, Ci W, Long M, Zhou B, Wu Y, et al. (2010) Synthesis of Visible-light Responsive Graphene oxide/TiO₂ Composites with p/n Heterojunction. *ACS Nano* 4: 6425-6432.